JOURNAL OF Materials CHEMISTRY

On sorption and thermal properties of the zirconium phosphate fluoride $[(H_2en)_{0.5}][Zr_2(PO_4)_2(HPO_4)F]\cdot H_2O$

Michael Feist,[a] Martin Wloka,[a] Matthias Epple,[b] Ekkehard Post[c] and Erhard Kemnitz*[a]

[a]*Institut für Chemie der Humboldt Universität zu Berlin, Hessische Str. 1–2, D-10115 Berlin, Germany*

[b]*Institut für Anorganische und Angewandte Chemie der Universität Hamburg, Germany*

[c]*Netzsch Gerätebau GmbH, Selb, Germany*

The thermal behavior of the title compound (ZrPO-1) has been investigated using conventional thermal analysis techniques as well as coupled TG–MS, TPD and XRD. Owing to the channel structure, ZrPO-1 reveals zeolitic properties in the dehydration range (up to 200 °C) whereas the removal of the organic template above 400 °C results in a complete loss of the sorptive activity. Water may be substituted by ammonia which is then released in two well separated steps at *ca.* 150 and 300 °C, respectively. The stronger differentiation of the water sites by the ammonia sorption allows attribution of the desorption ranges to the channels and the cavities, respectively, that exist in the structure. X-Ray characterization of the product after removal of the template above 400 °C did not yield any known zirconium phosphate or oxide. EXAFS measurements show that no significant changes occur in the short-range order around zirconium neither by dehydration nor by annealing. However, the environment of zirconium becomes increasingly disordered at higher temperatures.

Recently, we reported the crystal structure of $[(H_2en)_{0.5}][Zr_2(PO_4)_2(HPO_4)F]\cdot H_2O$ which was designated ZrPO-1.[1] It represents the first zirconium homologue to the well known microporous aluminium phosphate zeolites, ($AlPO_4$-*n*).[2] The structures of further representatives of the ZrPO-*n* type which have been obtained with different templates will be described elsewhere.[3]

The structure of ZrPO-1 contains a three-dimensional arrangement of zirconium octahedra (one ZrO_6 and one ZrO_5F), and phosphate tetrahedra [one $PO_3(OH)$ and two PO_4] being connected *via* common oxygen atoms. Both fluorine atoms and OH groups are terminal and, therefore, do not participate in the polyhedra connectivity. The eight-membered cyclic arrangement of alternating octahedra and tetrahedra forms holes with a diameter of approximately 6.5 Å. Channels in the *y*-direction exist in the structure, that form bottlenecks owing to the eight-membered polyhedra arrangement (Fig. 1).

The organic template, *i.e.* the ethylenediammonium cation, occupies these channels between two bottlenecks. As schematically shown in Fig. 2, the cation is disordered between two positions around an inversion center, which results in an empty space remaining in the channel, whereas the nitrogen atoms adopt identical positions. They are linked to the fluorine atoms of the ZrO_5F octahedra *via* hydrogen bridges. Fig. 1 further demonstrates that the water molecules occupy two crystallographically different sites. For each orientation of the template cation, the remaining empty space is occupied by one water molecule, which is disordered as well (occupancy factor 0.5). Another water molecule being situated on the twofold axis is not disordered (occupancy factor 0.5 as well). Within a small cavity, it is tetrahedrally linked to the inorganic frame *via* four hydrogen bridges: two times with a donor, and two times with an acceptor function.

Our study of the thermal behavior of ZrPO-1, assumed to exhibit zeolitic properties, has been directed by the following aspects. First, the dehydration and rehydration processes and their reversibility with special regard to the two different bonding situations of the water; secondly, the possible substitution of water in the channel by other molecules of comparable size, and, thirdly, the chemical and structural changes that are caused by the thermally induced removal of the template.

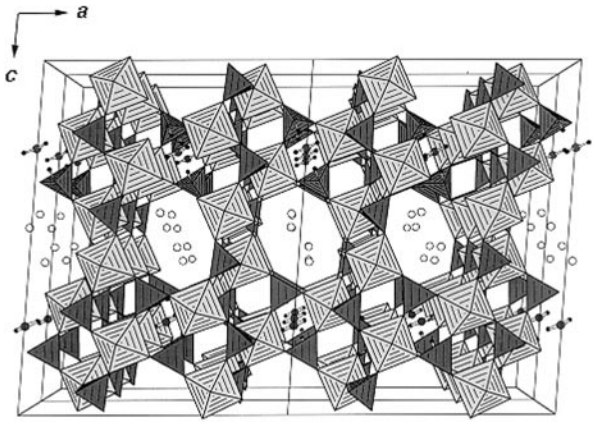

Fig. 1 Crystal structure of $[(H_2en)_{0.5}][Zr_2(PO_4)_2(HPO_4)F]\cdot H_2O$ (ZrPO-1). Half of the water molecules are situated in the tetragonal cavities (shadowed circles), the other half in the eight-membered ring channels. Owing to the disordering of the template cations, which are not shown here for better legibility (see Fig. 2), the water molecules in the channels are disordered as well (empty circles, both positions shown).

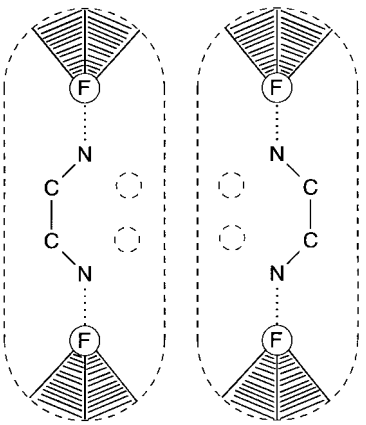

Fig. 2 Schematic view of the disordering of the ethylenediammonium cation in the channels of ZrPO-1 (view in *y* direction; dotted circles: oxygen positions of the disordered water molecule)

Experimental

Synthesis

The preparation of ZrPO-1, which is described in more detail elsewhere,[1] has been performed by hydrothermal synthesis (180 °C) from an aqueous solution of $ZrOCl_2 \cdot 8H_2O$, ethylenediamine monohydrate, 40% HF and H_3PO_4.

Thermal investigations

We have used a conventional DTA–TG apparatus (Netzsch STA 429) as well as a TG–MS coupling (Netzsch STA 409/skimmer system).[4] The macro sample holder system with platinum crucibles was used (Pt/PtRh10 thermocouples; α-Al_2O_3 as reference; 100 ml Ar min^{-1} for the DTA–TG, 100 ml He min^{-1} for the TG–MS measurements; $\beta = 5$ K min^{-1}; sample mass *ca.* 100 mg). For the enthalpimetric evaluation of the DTA curves (maximal precision of 10–12%) the measuring system was calibrated according to literature recommendations.[5,6] The TPD studies were performed with a Perkin Elmer FTIR spectrometer PE 2000 (TGS detector, resolution 4 cm^{-1}, 70 ml N_2 min^{-1}). A mixture of N_2 : NH_3 (*ca.* 3 : 1) was used for the NH_3 sorption. In order to avoid additional surface NH_3 sorption, every loading was followed by one hour flushing in pure N_2. For the X-ray characterization, a powder diffractometer XRD 7 (Seiffert PM, Freiberg, Germany) was used.

EXAFS measurements

X-Ray absorption fine-structure spectroscopy (EXAFS) was carried out at the Hamburger Synchrotronstrahlungslabor (HASYLAB) at Deutsches Elektronen-Synchrotron (DESY), Hamburg, at beamline X (ROEMO II). The DORIS III storage ring was operated at 4.5 GeV positron energy and currents of 50–120 mA. The incoming synchrotron beam was monochromatized by a Si(311) double-crystal monochromator. Experiments were performed at the Zr K-edge (*ca.* 17 999 eV) in transmission mode at room temperature. The ground samples were thoroughly mixed with boron nitride and pressed to a pellet. For quantitative data evaluation we used the programs AUTOBK and FEFFIT of the University of Washington package.[7] Theoretical standards were computed with the program FEFF 5.04[8] using the crystal structure of $[(H_2en)_{0.5}][Zr_2(PO_4)_2(HPO_4)F] \cdot H_2O$.[1] All fits were carried out with k^3-weighted data using a k-range of 2–14 $Å^{-1}$ and an R-range of 0.6–6.6 Å. The amplitude reduction factor S_0^2 was fixed to 1.22 as this value was obtained from fits of the pure educt compound with constant coordination number. One zero-energy correction [$E_0 = +12.1(6)$ eV] was chosen for the first four shells (6 O/F, 5.5 P, 6.125 O, 2.75 O) and another [$E_0 = -2.8(5)$ eV] for the zirconium shell at 6.62 Å. In order to reduce the number of fit parameters, the same Debye–Waller factor was chosen for the three oxygen shells.

Results and Discussion

Thermoanalytical and absorption studies

Two well separated endothermal effects, correlated to mass loss steps, characterize the thermal behavior of ZrPO-1 under normal pressure in argon [Fig. 3(*a*)]. With respect to the above described structural features, the first mass loss is attributed to dehydration (up to 200 °C) where the observed mass loss of 3.5% corresponds well to the value calculated for 1 mol H_2O (3.36%). Consequently, the second step (350–450 °C) is due to the removal of the template but, looking at the low mass loss of 3.5% (Δm_{calc} 9.35% for 0.5 en·2HF, or 5.62% for 0.5 en) and the curve shape (no plateau and not complete at 450 °C), it is rather incomplete or, at least, more complicated than a simple evaporation process.

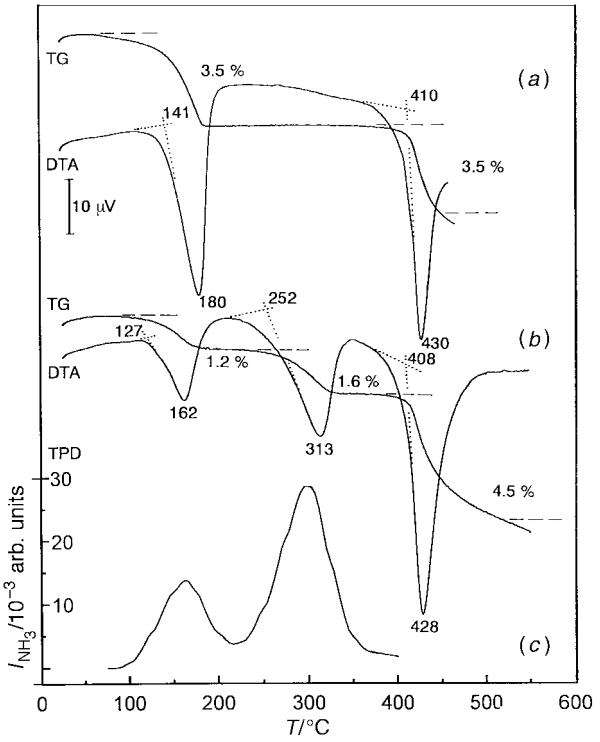

Fig. 3 STA curves for the dehydration and the template step: (*a*) of non-treated ZrPO-1; (*b*) of a dehydrated (200 °C) sample followed by NH_3 sorption (*cf.* Table 1); (*c*) NH_3 TPD curve of sample (*b*)

In accordance with the idea of different water sites (Fig. 1), the ion current (I.C.) curves for m/z 17 and 18 reveal a discontinuous shape (Fig. 4) whereas the DTA curves do not show any shoulder or double peak [Fig. 3(*a*)]. Additional information on the dehydration step is obtained from the DTA and DTG traces in Fig. 5, which correspond to the manifold sample treatment described in Table 1. The reversibility of the dehydration as well as the ammonia sorption properties of the dehydrated phase clearly reveal the zeolitic character of ZrPO-1. Upon rehydration, the original bonding situation of water is recovered. This may be deduced from the X-ray powder pattern (see next section) as well as from the identity of signal shape and area ($\Delta_{dehyd}H$ *ca.* 51 kJ mol^{-1}) for the first to third dehydration steps (*cf.* Table 1 for details of the experimental procedure). The slightly enhanced mass gain upon rehydration may be explained by the higher sorption activity of the primarily dehydrated phase. When it is reheated without preflushing in argon, this surface adsorbed water is released, causing a small separate effect [Fig. 5(*b*)], whereas the true dehydration effect has the same shape and area as for the first heating. On the contrary, if a rehydrated sample is exposed to a dry argon flow (20 h, 25 °C), the adsorbed water is released, and the pre-effect does not occur upon heating [Fig. 5(*c*)].

The interpretation of the second endothermal reaction range turned out to be more complicated even with the use of TG–MS measurements. The curves in Fig. 4 show that the template removal step is primarily caused by the release of carbon-containing species from the ethylenediammonium cation. Taking into account earlier findings on the thermal behavior of the related triethylenediammonium compounds, *e.g.* of chlorometalates like $(H_2trien)[CoCl_4]$,[9] several mass spectral peaks may be readily attributed to fragments of the template cation. However, the whole decomposition process, unfortunately, is rather unspecific because several processes are overlaying each other in this temperature range. This produces the quasi-continuum of higher mass peaks (*cf.* Fig. 4) and does not allow postulation of any main reaction for the decay.

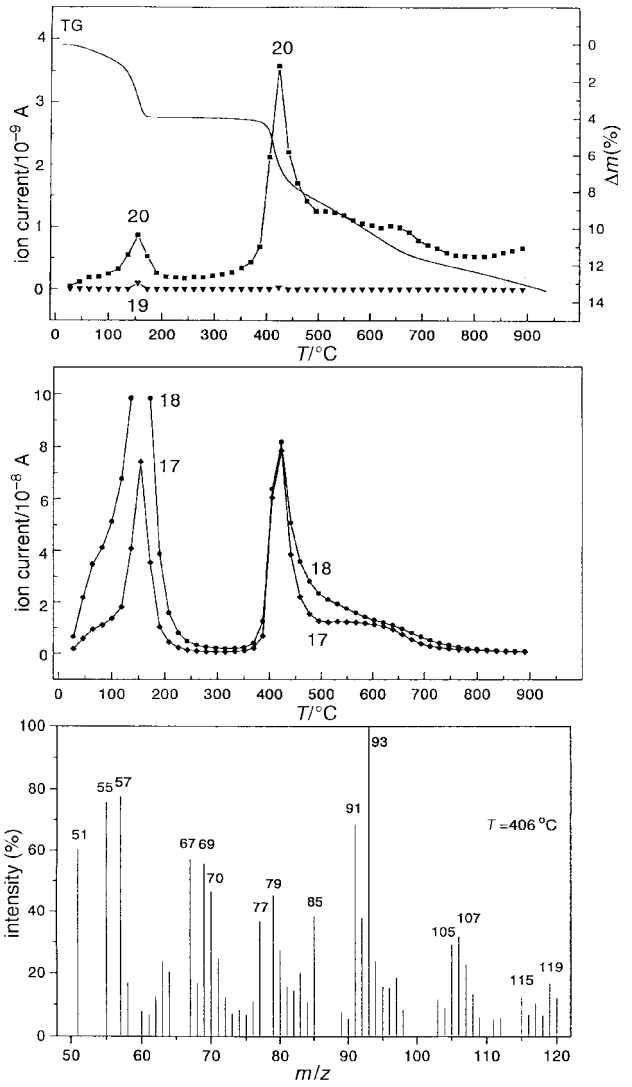

Fig. 4 TG–MS curves of ZrPO-1 (ion current curves for *m/z* 17,18,19,20 and mass number scan at the beginning of the template step)

The template removal step consists of a first partial step with bigger substance flow (340–450 °C) and a remarkably retarded following step (up to 700 °C), and is not completely finished even above 900 °C. Under these dynamic conditions, either the organic template is partially retained by the solid phase or it reacts secondarily with the zirconium phosphate matrix to yield further volatile products. Obviously, no mass-constant phase, *e.g.* related to a zirconium oxide, is formed here as might have been expected.

Nevertheless, some further qualitative details may be deduced from the TG–MS data. First, it may be seen that water is released not only in the dehydration step but is also formed during the template decomposition. This may be explained by condensation reactions of two neighbouring P—OH groups. Secondly, the formation of ammonia in the second TG step is observed when considering the I.C. intensity ratio for *m/z* 17 : 18. The mass loss corresponds to that expected only for water in the first TG step but, owing to a certain contribution by ammonia, it is much higher in the second step. Thirdly, HF liberation (*m/z* 19, 20) takes place predominantly in the template removal step. That means that not only the organic component is removed from the channels but the zirconium phosphate matrix is attacked as well and the sorptive activity of the Zr–P–O phase(s) disappears. The small amounts of HF detected in the first TG step were attributed to surface adsorbed HF which is rationalized by the conditions of the hydrothermal synthesis.

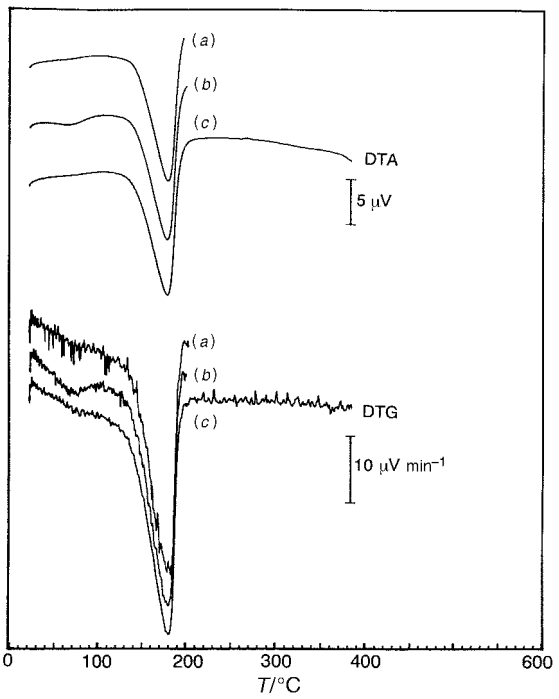

Fig. 5 DTA and DTG curves for the dehydration range of ZrPO-1 for repeated dehydration/rehydration cycles corresponding to the stepwise sample treatment described in Table 1: (*a*) first dehydration (step 1); (*b*) second dehydration (step 4); (*c*) third dehydration (step 8)

The disappearance of the zeolitic properties of ZrPO-1 is expressed by the fact that neither water nor ammonia may be absorbed by the product phase which is formed during the template removal step (Table 1). The small amount of water taken up at 25 °C subsequent to the template removal step is only surface adsorbed. Therefore, the small mass loss of *ca.* 1% that appears on reheating has no corresponding DTA signal. An identically treated sample, cooled in ammonia, does not show any mass loss upon reheating under argon.

A completely different situation is found when ZrPO-1 is only dehydrated (200 °C) and is then cooled to room temperature in an ammonia flow. Upon reheating, two well separated TG steps [Fig. 3(*b*),(*c*)] indicate differently bound NH_3 molecules which have been absorbed by the host structure ($\Delta m_{NH_3} \approx \Delta m_{H_2O}$!), possibly onto the positions that were originally occupied by the two different types of water molecules. With NH_3, the second desorption maximum is observed at a much higher temperature (ΔT *ca.* 150 K) than the first one which is in the dehydration range. This shift is too large for the assumption that only variations in the hydrogen bonding would differentiate the water sites, now being substituted by ammonia molecules. The changes caused by the ammonia sorption seem to be more profound to rationalize the considerable shift of the second desorption peak. One possible reason is the formation of NH_4^+ ions, which could explain a stronger fixation of ammonia in the solid *via* additional coulomb interactions rather than just hydrogen bonding. The formation of ammonium ions is possible if one takes into account the terminal OH groups existing in the structure of ZrPO-1. Owing to the greater basicity of ammonia relative to water the OH groups can act as proton donors to form NH_4^+ ions.

Thus, the two desorption maxima could be interpreted in terms of, first, hydrogen bound NH_3 molecules, which would be quite analogous to the situation of water in the structure of ZrPO-1. Secondly, NH_4^+ ions, which are formed *via* reaction between OH groups and NH_3, would be more strongly retained in the structure and explain the liberation of NH_3 at higher temperatures. That means that we are able to attribute the

Table 1 Procedure of sample treatment for three different samples of ZrPO-1[a]

step	process	temperature program[b]	Δm (%)
1	dehydration	↑200 °C in Ar	−3.6
2	cooling	↓25 °C in Ar	—
3	rehydration	12 h at 25 °C in moist air	+4.0
4	dehydration	↑200 °C in Ar	−0.6 and −3.3
5	cooling	↓25 °C in Ar	—
6	rehydration	43 h at 25 °C in moist air	+4.0
7	dry gas flow	20 h at 25 °C	0 (!)
8	dehydration and further heating	↑460 °C in Ar	−3.5 (H_2O) and −3.5 (template)
9	cooling	↓25 °C in Ar	—
10	rehydration	20 h at 25 °C in moist air	+1.0
11	heating	↑460 °C in Ar	−1.0
1	dehydration	↑200 °C in Ar	−3.6
2	NH_3 absorption	↓25 °C in NH_3	+2.9
3	desorption	↑370 °C in Ar (TPD)	−1.2 and −1.6
1	dehydration and further heating	↑ 460 °C in Ar	−3.5 (H_2O) and −3.5 (template)
2	NH_3 absorption	↓180 °C in Ar followed by ↓25 °C in NH_3	—
3	heating	↑200 °C in Ar	0 (!)

[a]Steps 1–11 performed in a single experimental run on the thermobalance, the ammonia sorption in a preparative scale followed by the STA measurement. [b]↑=heating, ↓=cooling.

first desorption peak to channel sites whereas the second peak corresponds to cavity sites.

Structural investigations

The structural changes caused by the dehydration yield powder diagrams (Fig. 6) which are quite similar to the educt phase, but not so readily assigned. However it can be deduced that the rehydrated phase is identical with the educt state. Meanwhile, we succeeded in preparing a single crystal of the dehydrated phase for a crystal structure analysis, the evaluation of which is underway. The following template step, as already discussed above, effects deeper chemical and structural changes of ZrPO-1 resulting in a completely different powder pattern. Our attempts for an indexation or an interpretation in terms of known crystalline phases existing in the Zr–O–P system failed, which led us to investigate the structural changes by EXAFS measurements.

Two different crystallographic positions exist for zirconium. Surrounding shells were computed for both positions to derive the average zirconium environment. Zirconium is surrounded by 0.5 fluorine atom (1.99 Å), 5.5 oxygen atoms (2.02–2.10 Å), 5.5 phosphorus atoms (3.34–3.55 Å), 6.125 oxygen atoms (3.81–4.02 Å) and 2.75 oxygen atoms (4.08–4.14 Å). Above 4.14 Å, a number of overlapping shells of light backscatterers (O, N, C) are present. Furthermore, there are zirconium neighbors at 4.85 Å ($N=1$), 5.1–5.25 Å ($N=3$), 5.45 Å ($N=1.5$) and 6.62 Å ($N=4$).

It was not possible to separate fluorine and oxygen in the first neighboring shell owing to almost identical backscattering behavior and distance. Therefore we combined the fluorine shell and the first oxygen shell into one oxygen shell with $N=6$ at 1.99–2.10 Å. The phosphorus atoms were combined into a single shell. The next oxygen shells ($N=6.125$ and 2.75) were also fitted. However, it should be kept in mind that higher shells are influencing the third oxygen shell. Additionally, multiple scattering paths come into play above $R=3.5$ Å. As an indicator for long-range order we used a distinct shell of four zirconium atoms at 6.62 Å. No other shells were included into the fit.

As expected, the main structural framework did not change upon dehydration. Only small changes are visible even upon annealing at 800 °C. This is seen from the close similarity of EXAFS Fourier transforms as shown by visual inspection (Fig. 7 and 8). Consequently, the coordination numbers were fixed to their theoretical (crystallographic) values during the fits. The results of the fits (average of two EXAFS scans at room temperature) are listed in Table 2.

Two main results can be summarized as follows: all five shells are present in the four samples and the interatomic distances remain the same within the experimental scatter.

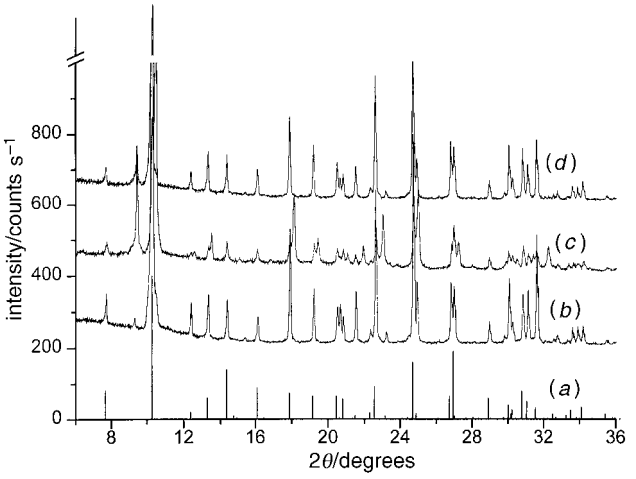

Fig. 6 Calculated (*a*) and experimental powder diffractogram of ZrPO-1 (*b*) compared with those of a dehydrated (200 °C) (*c*) and a rehydrated sample (*d*)

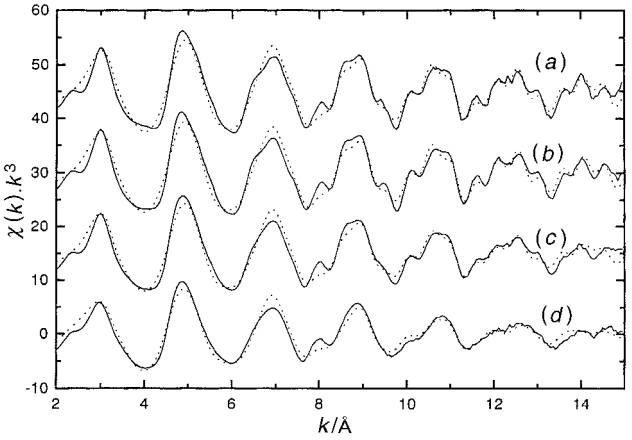

Fig. 7 k^3-weighted Zr K-edge EXAFS functions $\chi(k)$ for ZrPO-1: (*a*) untreated, (*b*) dehydrated at 200 °C, (*c*) heated to 400 °C, and (*d*) heated to 800 °C, template removed

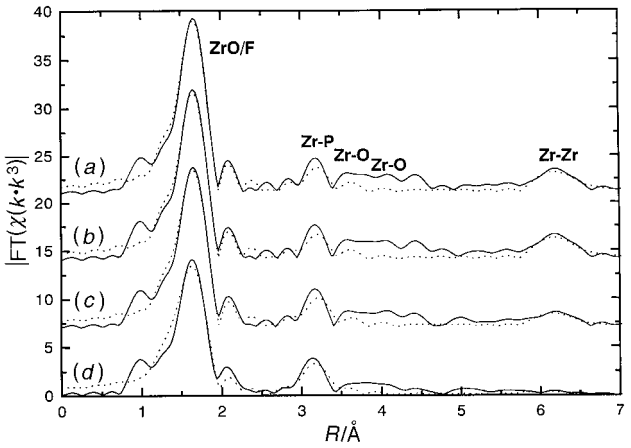

Fig. 8 Fourier-transform magnitudes of ZrPO-1 after different thermal treatments (*cf.* Fig. 6). The coordination of zirconium remains unchanged up to $R \approx 4$ Å; however, the disorder increases as visible from the decreasing height of the Zr–O/F peak at 2.1 Å. The Zr–Zr shell at 6.6 Å almost vanishes upon heating to 800 °C, indicating a structural change. The data are not corrected for phase shifts.

This illustrates that the short-range order around zirconium is not changed by dehydration and annealing. However, the structural disorder, as represented by the Debye–Waller factors, increases, indicating a slow breakdown of the zeolitic structure. This change is most obvious in the Zr—Zr shell at 6.62 Å. If the coordination number is fixed to four as in the original structure, the Debye–Waller factor almost quadruples in the sample heated to 800 °C. If the Debye–Waller factor is kept constant at 2.6×10^{-3} Å^2 and the coordination number is varied, we obtain $N = 2.3$ (400 °C) and $N = 0.6$ (800 °C). The strong correlation between N and σ^2 prevents the exact determination of N, but it is quite clear that the environment of zirconium becomes increasingly disordered at higher temperature. It was very difficult to fit the phosphorus shell. The Zr—P distance was found to be too large, and also an unreasonably high Debye–Waller factor was found. We ascribe these problems to a strong correlation between the Zr—P shell and the neighboring Zr—O shell.

Despite the structural similarity, the template effect and the thermal behavior of ZrPO-1 differs from that of typical representatives of the neighbouring AlPO family, *e.g.* that of the VPI-5 type which represents a wide-pore 18-ring aluminium phosphate.[10] Upon dehydration (120 °C !) it rapidly rearranges to another intact AlPO structure, AlPO-8, if the compound is prepared in the presence of dipropylamine. On the other hand, the VPI-5 structure remained stable if the hydrothermal synthesis was performed in the presence of dipentylamine.[11] For the known ZrPOs, a template effect governing the thermal stability of the metal phosphate fluoride framework is not observed with the main structural motif and reversible hydration/dehydration behavior remaining unchanged.

Conclusions

ZrPO-1 shows zeolite-like properties at low temperatures. This is evidenced by the conservation of the channel structure of the zirconium phosphate framework upon dehydration, by its reversibility, and by the possibility of substituting water by ammonia. On the other hand, a complete loss of the sorptive activity is observed when the template is thermally removed from the ZrPO-1 structure. The channel structure collapses but the short-range order of the Zr atoms remains nearly unchanged which might indicate that the formed structure is very similar. However, this is not necessarily the case since the short-range arrangement of layered zirconium phosphates is, to some degree, similar to the short-range constitution of 3D ZrPOs.[3] It is not clear as yet whether the product after removal of the template represents a single phase system or a mixture of various zirconium phosphates and/or oxides. Therefore, further structural investigations of the detemplated phase are required.

The support of Dr. W.-D. Emmerich (Netzsch Gerätebau GmbH, Germany) who enabled the TG–MS investigations to be carried out is gratefully acknowledged. We thank Larc Tröger (Hamburg) for experimental assistance, and we are grateful to HASYLAB at DESY for generous allocation of beamtime. The financial support by the Deutsche Forschungsgemeinschaft (DFG) and the Fonds der Chemischen Industrie (FCI) is also gratefully acknowledged.

Table 2 Results of EXAFS experiments carried out at the zirconium K-edge for ZrPO-1 after different thermal treatments (coordination numbers fixed to their crystallographic values for hydrated and dehydrated phases)

	sample treatment			
	25 °C (untreated)	200 °C (dehydrated)	400 °C (beginning of template step)	800 °C (template removed)
1st shell: 6 O/F				
N^a	6	6	6	6
R/Å	2.06(2)	2.08(2)	2.08(2)	2.07(2)
$\sigma^2/10^{-3}$Å^2	4.1	5.2	5.4	7.2
2nd shell: 5.5 P				
N^a	5.5	5.5	5.5	5.5
R/Å	3.72(2)	3.85(2)	3.72(2)	3.66(2)
$\sigma^2/10^{-3}$ Å^2	7.8	95.5	8.9	6.2
3rd shell: 6.125 O				
N^a	6.125	6	6	6
R/Å	3.74(2)	3.86(2)	3.74(2)	3.66(2)
4th shell: 2.75 O				
N^a	2.75	2.5	2.5	2.5
R/Å	4.06(2)	4.04(2)	4.05(2)	4.03(2)
higher shell: 4 Zr				
N^a	4	4	4	4
R/Å	6.63(2)	6.62(2)	6.62(2)	6.63(2)
$\sigma^2/10^{-3}$Å^2	2.6	2.9	4.8	10.5

[a]Fixed.

References

1 E. Kemnitz, M. Wloka, S. Trojanov and A. Stiewe, *Angew. Chem.*, 1996, **108**, 2809.
2 S. T. Wilson, B. M. Lok, C. A. Messina, T. R. Cannan and E. M. Flanigan, *J. Am. Chem. Soc.*, 1982, **104**, 1146.
3 M. Wloka, S. I. Troyanov and E. Kemnitz, *J. Solid State Chem.*, in press.
4 T. Rampke, W. D. Emmerich, E. Post and L. Giersig, *J. Therm. Anal.*, 1996, **47**, 633.
5 K. Heide, *Dynamische Thermische Analysenmethoden*, VEB Deutscher Verlag für Grundstoffindustrie, Leipzig, 1982.
6 H. K. Cammenga, W. Eysel, E. Gmelin, W. Hemminger, G. W. H. Höhne and S. M. Sarge, *Thermochim. Acta* , 1993, **219**, 333.
7 E. A. Stern, M. Newville, B. Ravel, Y. Yacoby and D. Haskel, *Physica B*, 1995, **208–209**, 117.
8 J. J. Rehr, R. C. Albers and S. I. Zabinsky, *Phys. Rev. Lett.*, 1992, **69**, 3397.
9 M. Feist, R. Kunze, D. Neubert, K. Witke and E. Kemnitz, *J. Therm. Anal.*, 1997, **49**, 635.
10 M. E. Davis, C. Saldarriaga, C. Montes, J. M. Garces and C. Crowder, *Nature* (*London*), 1988, **331**, 698.
11 J. O. Perez, P. Jen Chu and A. Clearfield, *J. Phys. Chem.*, 1991, **95**, 9994.

Paper 7/05459I; *Received* 28*th July*, 1997